

795 nm 大功率外腔半导体激光器的研究

张薇^{1,2}, 仲莉^{*}, 张德帅^{1,2}, 吴霞¹, 倪羽茜¹, 刘素平¹, 马晓宇¹¹中国科学院半导体研究所光电子器件国家工程研究中心, 北京 100083;²中国科学院大学材料科学与光电技术学院, 北京 100049

摘要 采用超极化惰性气体的磁共振成像技术可大大提高肺部影像成像质量,其中自旋交换光泵作为超极化惰性气体的关键,通常是对碱金属铷进行泵浦,为获得较好的泵浦效率,要求泵浦源具有窄光谱宽度和高功率的特点。针对这一需求,提出以体布拉格光栅(VBG)作为外腔反馈元件的 795 nm 窄谱宽外腔半导体激光器设计,并对 VBG 的外腔锁模稳定性进行了分析讨论,最终实现了功率为 6.36 W,谱宽低至 0.036 nm 的 795.245 nm 单管外腔激光输出,为实现大功率的单管外腔半导体激光器奠定基础。

关键词 激光器; 外腔半导体激光器; 体布拉格光栅; 窄谱宽; 锁模

中图分类号 TN248.4

文献标志码 A

DOI: 10.3788/AOS222014

1 引言

大功率半导体激光器(LD)具有体积小、功耗低、电光转换效率高^[1]等优点,被广泛应用于泵浦碱金属蒸气激光器、固体激光器、光纤激光器等^[2]。其中,794.7 nm 大功率半导体激光器常用于自旋交换光泵^[3-5]过程中对碱金属铷的泵浦,如何提高该过程的泵浦效率是研究人员关注的主要问题之一。目前,商用大功率半导体激光器的谱宽较宽,而碱金属原子在常温下的多普勒展宽线宽^[6-7]较窄仅有 0.05 nm,难以实现高效泵浦。为此,国内外研究人员主要采用面光栅或体布拉格光栅(VBG)作为外腔反馈元件,对半导体激光器的谱宽进行压窄,实现泵浦谱宽与原子吸收谱宽的匹配,以提高泵浦效率。

近年来,国内外基于光栅外腔结构的半导体激光器已有不少研究:Podoskin 等^[8]报道了一种基于 Littrow 型的面光栅外腔半导体激光器,可实现功率为 13 W、谱宽为 0.15 nm 的激光输出;刘荣战等^[9]采用 15% 衍射效率的体布拉格光栅进行外腔锁模,最大输出功率达 10.7 W,输出波长稳定在 888 nm,谱宽低至 0.3 nm;何林安等^[10]基于体布拉格光栅外腔结构,在工作电流为 10 A 的条件下,实现了功率为 10.1 W、谱宽为 0.06 nm 的 780 nm 激光输出;王渴等^[11]基于空间合束技术将 6 片单管增益芯片合束通过体布拉格光栅,激光输出功率达到 26.32 W 的同时谱宽低至 0.18 nm。在已有报道中,同时实现窄谱宽、大功率激光输出的研究较少,并且在大功率需求下,多数研究采

用巴条为内部增益结构^[12-13],存在光束质量较差^[14]、耦合难度较大等问题。

为满足自旋交换光泵中对泵浦源的需求,本文采用单管芯片为增益元件、体布拉格光栅为外腔反馈元件的结构,实现了功率为 6.36 W、谱宽低至 0.036 nm 的 795 nm 激光输出,器件性能同时满足大功率、窄谱宽特点,为实现大功率的单管外腔半导体激光器奠定基础。

2 基本原理及设计

外腔半导体激光器的基本原理^[15-17]如图 1 所示,外腔激光器输出模式包括增益芯片本身的内腔模以及外腔与增益芯片构成的外腔模,光学选频元件通过窄带滤波作用将具有一定带宽的光束反馈回增益芯片,再经增益饱和和模式竞争作用达到压窄谱宽的目的。为获得稳定的大功率、窄谱宽激光输出,本文采用体布拉格光栅作为光学反馈元件,体布拉格光栅由光敏玻璃材料制作^[18],温漂系数约为 0.01 nm/°C,阈值损伤为 1 kW/cm²,并且偏振不敏感,非常适合作为大功率外腔半导体激光器的反馈元件。

基于外腔反馈元件体布拉格光栅对器件外腔结构进行设计。本研究采用的 VBG 厚度为 6.0 mm,截面尺寸为 3.0 mm×2.0 mm,衍射效率峰值为 30%,图 2 为基于 VBG 结构参数绘制的 VBG 衍射效率与入射波长、入射光束角度理论关系图^[19]。如图 2(a)所示,VBG 的衍射效率峰值位于 795.245 nm 处,并受入射波长影响,因此所采用的增益芯片激光光谱需覆盖

收稿日期: 2022-11-18; 修回日期: 2022-12-21; 录用日期: 2023-01-29; 网络首发日期: 2023-02-07

通信作者: *zhongli@semi.ac.cn

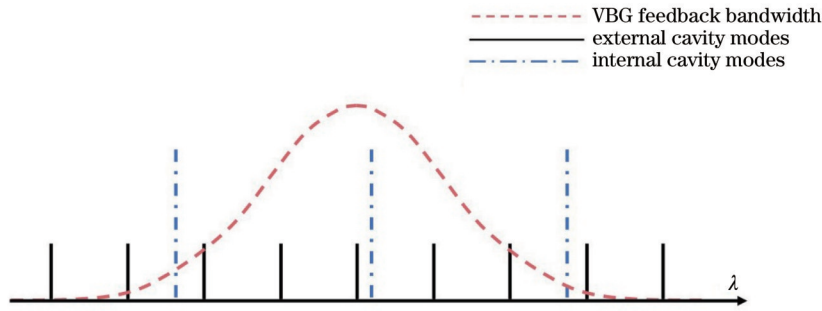


图1 半导体激光器外腔模式、内腔模式及 VBG 反馈带宽示意图

Fig. 1 Schematic diagram of external cavity mode, internal cavity mode, and VBG feedback bandwidth of semiconductor laser

VBG 的理论反射带宽。如图 2(b)所示, VBG 衍射效率受入射光束角度影响, 为使 VBG 发挥最佳衍射效率, 需在外腔结构中加入快轴准直透镜(FAC)和慢轴准直透镜(SAC)对光束的发散角进行整形。

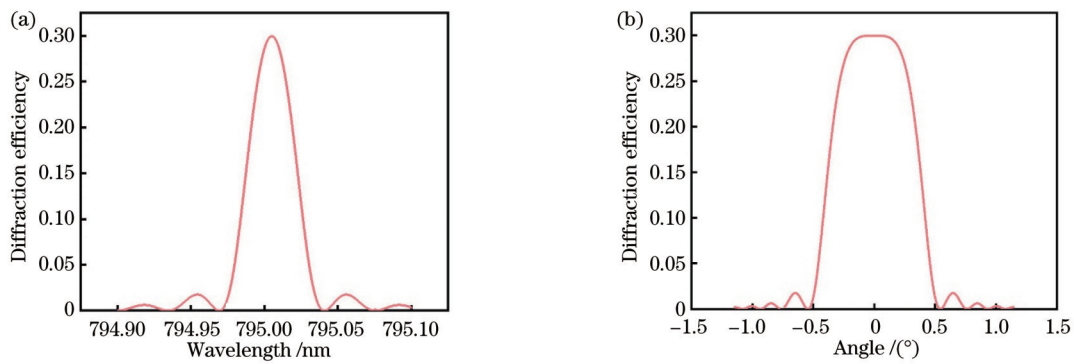


图2 体布拉格光栅衍射效率与入射波长、入射角度的关系。(a)入射波长;(b)入射角度

Fig. 2 Relationship between volume Bragg grating diffraction efficiency and incident wavelength and incident angle. (a) Incident wavelength; (b) incident angle

图3为实验装置示意图, 其中单管增益芯片为本实验室自主研发的大光腔激光器, 发光区尺寸为 $1.5 \mu\text{m} \times 100 \mu\text{m}$, 采用大光腔、宽发光截面的结构可以有效降低腔面处的光功率密度, 有利于高功率激光输出。为抑制增益芯片内腔模式对外腔激光器输出性能的影响, 需要对增益芯片前腔面进行增透处理, 采用 $\text{TiO}_2/\text{Al}_2\text{O}_3/\text{SiO}_2$ 膜系蒸镀反射率为 0.2% 的增透膜, 后腔面采用 $\text{Al}_2\text{O}_3/\text{Si}$ 膜系蒸镀反射率为 96% 的高

反膜。为便于进行温度控制, 通过焊料将增益芯片焊接到热沉上。外腔结构中采用 0.2 mm 焦距的 FAC) 和 12 mm 焦距的 SAC 对增益芯片激光束进行整形, 准直后的快、慢轴远场发散角经 CCD 测量分别为 0.9° (95%) 和 2.3° (95%)。实验测试中, 在 VBG 后放置分光片, 以便同时测量激光光束的光谱和功率, 激光光谱测量采用 Anritsu 公司的 MS9740B 光谱仪, 在 795 nm 处的光谱分辨率为 0.034 nm。

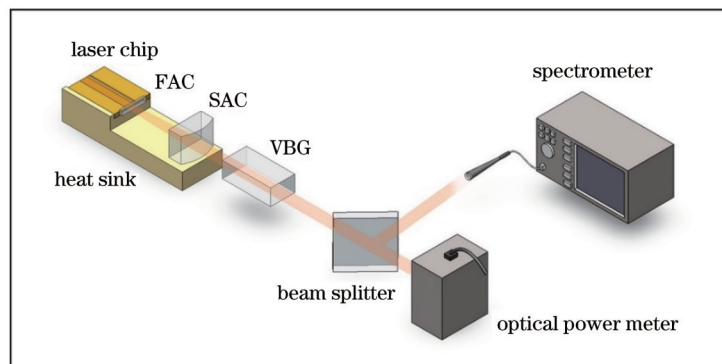


图3 实验装置示意图

Fig. 3 Schematic diagram of experimental device

3 实验结果及讨论

3.1 谱宽压窄实验

本研究中的增益芯片工作电流较大,在实现大功率激光输出的同时将产生大量的热,产热导致的温升势必会影响器件的输出性能,因此在实验中控制增益芯片工作温度为 $16\text{ }^{\circ}\text{C}$,以确保增益芯片输出稳定的激光。VBG 由夹具夹持放置于六维调整架上,通过监测光谱,调节 VBG 的位置及角度使经快慢轴透镜的光束准直入射光栅,以达到较好的谱宽压窄效果。

图 4 为在增益芯片驱动电流为 10 A 时,采用 VBG 对增益芯片进行锁模前后的激光输出光谱。增益芯片自由运行时的光谱呈多纵模、宽谱宽的特点,中心波长为 795.875 nm ,谱宽为 2.630 nm ,输出功率为 7.19 W ,经 VBG 滤波反馈作用后的激光中心波长锁定在 795.245 nm ,谱宽压窄至 0.036 nm ,输出功率为 6.36 W ,外腔耦合效率达到 88.5% 。由以上结果可知,VBG 作为外腔反馈元件不仅能够压窄半导体激光器的输出激光谱宽,还具有光束耦合效率高、损耗小的特点,可实现大功率激光输出。

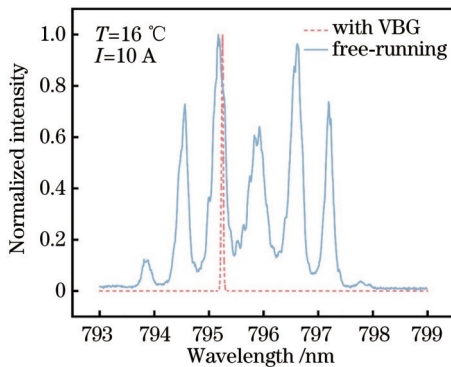


图 4 采用 VBG 对半导体激光器进行锁模前后的激光输出光谱
Fig. 4 Laser output spectrum of the semiconductor laser before and after mode locked by VBG

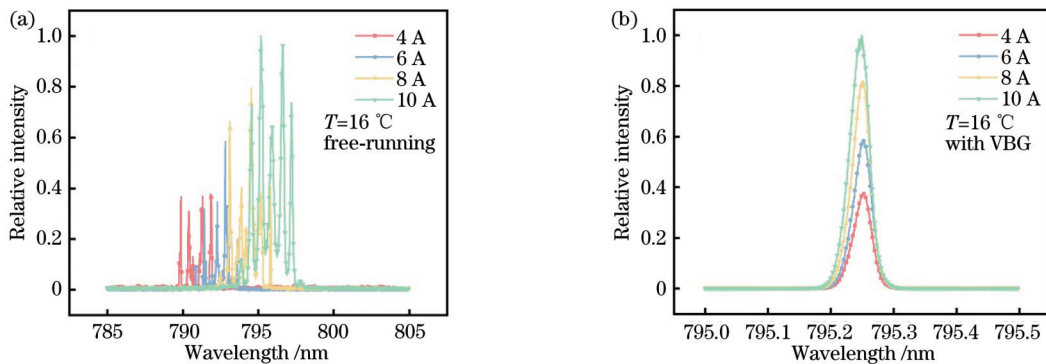


图 6 不同驱动电流条件下的光谱分析。(a)增益芯片自由运行光谱;(b)体光栅外腔半导体激光器光谱
Fig. 6 Spectral analysis under different driving current conditions. (a) Spectrum of gain chip free-running; (b) spectrum of external cavity semiconductor laser with VBG

图 5 为体布拉格光栅外腔半导体激光器的输出功率特性曲线,与增益芯片自由运行时的曲线相比,斜率效率由 0.96 W/A 下降至 0.87 W/A 。斜率效率下降主要是外腔结构损耗引起的,该损耗受快、慢轴准直透镜的镜面反射率及 VBG 对入射光束的角度选择性所影响,所以在外腔结构中采用镀有增透膜的非球面快、慢轴准直透镜可减缓斜率效率的降低。

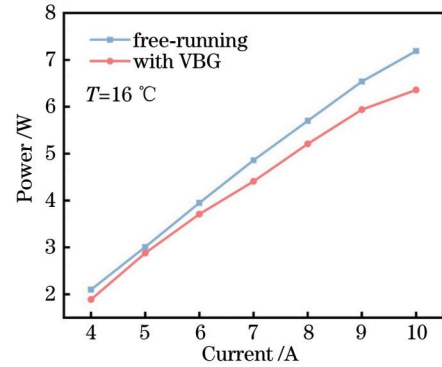


图 5 体布拉格光栅外腔半导体激光器输出功率特性曲线
Fig. 5 Output power characteristic curves of VBG external cavity semiconductor lasers

3.2 波长稳定性分析

然后,对体布拉格光栅外腔半导体激光器的波长稳定性进行实验分析。图 6(a)为单管增益芯片工作温度为 $16\text{ }^{\circ}\text{C}$ 时,不同驱动电流下的自由运行光谱,LD 的光谱呈现多纵模、宽谱宽的特点,谱宽约为 $2\sim 3\text{ nm}$,并且随着驱动电流的增大,LD 中心波长发生红移,波长对电流的漂移系数为 1 nm/A 。图 6(b)为采用体布拉格光栅设计的外腔半导体激光器的输出光谱,在恒定温度下,随着驱动电流的增加,外腔半导体激光器的中心波长可以稳定地锁定在 VBG 的反射中心波长上,波长随电流变化的漂移系数降低至 0.010 nm/A ,激光光谱宽度小于 0.036 nm ,即 VBG 的外腔反馈作用极大地改善了大功率半导体激光器本身谱宽,降低了波长随电流的漂移系数。

图 7 为体布拉格光栅外腔半导体激光器在驱动电流为 6 A 下,不同工作温度时的激射光谱。增益芯片自由运行时的温漂系数为 0.350 nm/°C,采用外腔反馈结构的半导体激光器温漂系数降低至 0.005 nm/°C,光谱宽度压窄至 0.036 nm,并且具有较好的边模抑制比。当增益芯片工作温度增大至 35 °C 时,外腔半导体激光器激射光谱出现侧峰,边模抑制比变差,此时增益芯片自由运行时的中心波长为 798.823 nm。出现此现象的原因主要归结于增益芯片中心波长与 VBG 中心波长偏差较大。本研究中的增益芯片中心波长与 VBG 反馈中心波长最大容差为 3.578 nm,当二者中心波长差值大于最大容差时,外腔激光器的波长锁定变差,出现侧峰,谱宽展宽至 0.058 nm。

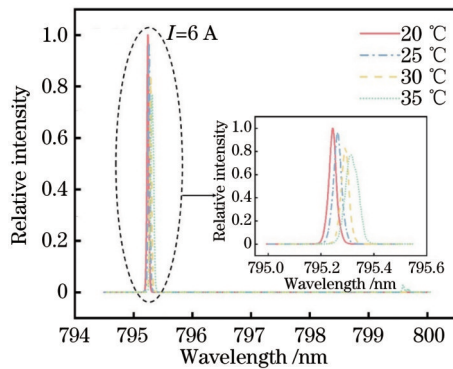


图 7 不同工作温度下外腔半导体激光器激射光谱

Fig. 7 Spectrum of external cavity semiconductor laser at different operating temperatures

基于以上对体布拉格光栅外腔半导体激光器波长稳定性的分析可知,VBG 作为半导体激光器的外腔反馈元件不仅可压窄谱宽,而且大大提升了器件输出波长的稳定性,器件在较大驱动电流及工作温度范围内具有稳定的激射光谱。因此,由增益芯片中心波长与 VBG 反馈中心波长的容差对外腔锁模的影响上可以得到,为保证器件在大功率激光输出下具有稳定的激射中心波长及较好的窄谱宽特性,增益芯片中心波长与 VBG 反馈中心波长在容差范围内需满足波长匹配。

VBG 外腔激光器的增益芯片中心波长与 VBG 反馈中心波长最大容差决定了器件的波长锁定能力,器件的最大容差与外腔反馈效率有关,受增益芯片前腔面反射率、VBG 衍射效率、各光学元件装调位置、透镜反射率等影响,在保证器件输出性能的条件下,进一步提升器件的稳定性需改变器件各参数至最佳值。

4 结 论

本文采用体布拉格光栅作为光学反馈元件进行了外腔半导体激光器的研制,对不同驱动电流、工作温度下的器件输出光谱进行了稳定性分析,在满足增益芯片中心波长与体布拉格光栅反馈中心波长匹配的条件下,最终实现了输出功率达到 6.36 W,谱宽低至

0.036 nm,外腔耦合效率达到 88.5% 的 795.245 nm 单管体布拉格光栅外腔半导体激光器输出。

参 考 文 献

- [1] 宁永强,陈泳屹,张俊,等.大功率半导体激光器发展及相关技术概述[J].光学学报,2021,41(1):0114001.
Ning Y Q, Chen Y Y, Zhang J, et al. Brief review of development and techniques for high power semiconductor lasers [J]. Acta Optica Sinica, 2021, 41(1): 0114001.
- [2] 李明月,何君.国外军用大功率半导体激光器的发展现状[J].半导体技术,2015,40(5):321-327.
Li M Y, He J. Development situations of high power semiconductor laser for military applications in advanced countries[J]. Semiconductor Technology, 2015, 40(5): 321-327.
- [3] Roos J E, McAdams H P, Kaushik S S, et al. Hyperpolarized gas MR imaging: technique and applications[J]. Magnetic Resonance Imaging Clinics of North America, 2015, 23(2): 217-229.
- [4] 杨昊,王科,涂宁,等.超极化¹²⁹Xe 人体肺部磁共振成像[J].武汉大学学报(医学版),2017,38(4):582-586.
Yang H, Wang K, Tu N, et al. Hyperpolarized ¹²⁹Xe MRI for human lung[J]. Medical Journal of Wuhan University, 2017, 38(4): 582-586.
- [5] 赵修超,孙献平,袁亚平,等.超极化气体氙-129的低场NMR测量[J].波谱学杂志,2016,33(3):458-467.
Zhao X C, Sun X P, Yuan Y P, et al. Measuring polarization of hyperpolarized xenon-129 gas with low-field NMR[J]. Chinese Journal of Magnetic Resonance, 2016, 33(3): 458-467.
- [6] 田景玉,张俊,彭航宇,等.用于碱金属蒸汽激光器泵浦的窄线宽 780 nm 半导体激光源[J].发光学报,2019,40(9):1123-1129.
Tian J Y, Zhang J, Peng H Y, et al. 780 nm diode laser source with narrow linewidth for alkali metal vapor laser pumping[J]. Chinese Journal of Luminescence, 2019, 40(9): 1123-1129.
- [7] 刘泽金,王红岩,许晓军.高能半导体泵浦气体激光器[J].中国激光,2021,48(4):0401001.
Liu Z J, Wang H Y, Xu X J. High energy diode pumped gas laser[J]. Chinese Journal of Lasers, 2021, 48(4): 0401001.
- [8] Podoskin A, Golovin V, Gavrina P, et al. Ultrabroad tuning range (100 nm) of external-cavity continuous-wave high-power semiconductor lasers based on a single InGaAs quantum well[J]. Applied Optics, 2019, 58(33): 9089-9093.
- [9] 刘荣战,蒋威,宋健.体布拉格光栅外腔半导体激光器温度特性研究[J].光子·激光,2022,33(12):1263-1270.
Liu R Z, Jiang W, Song J. Research on temperature characteristics of VBG external cavity semiconductor laser[J]. Journal of Optoelectronics·Laser, 2022, 33(12): 1263-1270.
- [10] 何林安,周坤,张亮,等.大功率 780 nm 半导体激光器的设计与制备[J].强激光与粒子束,2021,33(9):091001.
He L A, Zhou K, Zhang L, et al. Fabrication of high-power semiconductor laser with wavelength-locked at 780 nm[J]. High Power Laser and Particle Beams, 2021, 33(9): 091001.
- [11] 王渴,韩金樑,梁金华,等.窄线宽蓝光半导体激光器研究[J].中国激光,2023,50(10):1001004.
Wang K, Han J L, Liang J H, et al. Research on narrow linewidth blue semiconductor laser[J]. Chinese Journal of Lasers, 2023, 50(10): 1001004.
- [12] 李志永,谭荣清,徐程,等.用于铷蒸汽激光泵浦的窄线宽阵列半导体激光器[J].强激光与粒子束,2013,25(4):875-878.
Li Z Y, Tan R Q, Xu C, et al. Laser diode array with narrow linewidth for rubidium vapor laser pumping[J]. High Power Laser and Particle Beams, 2013, 25(4): 875-878.
- [13] Gourevitch A, Venus G, Smirnov V, et al. Continuous wave, 30 W laser-diode bar with 10 GHz linewidth for Rb laser pumping[J]. Optics Letters, 2008, 33(7): 702-704.

- [14] Yu J H, Guo L, Wu H L, et al. High brightness beam shaping and fiber coupling of laser-diode bars[J]. *Applied Optics*, 2015, 54(11): 3513-3516.
- [15] Detoma E, Tromborg B, Montrosset I. Frequency and time domain analysis of an external cavity laser with strong filtered optical feedback[J]. *Proceedings of SPIE*, 2004, 5452: 283-290.
- [16] Fischer A P A, Andersen O K, Yousefi M, et al. Experimental and theoretical study of filtered optical feedback in a semiconductor laser[J]. *IEEE Journal of Quantum Electronics*, 2000, 36(3): 375-384.
- [17] Sun H, Menhart S, Adams A. Calculation of spectral linewidth reduction of external-cavity strong-feedback semiconductor lasers[J]. *Applied Optics*, 1994, 33(21): 4771-4775.
- [18] 程灿, 辛国锋, 封惠忠, 等. 连续工作的体布拉格光栅外腔半导体激光器的温度特性[J]. *中国激光*, 2008, 35(1): 27-30. Cheng C, Xin G F, Feng H Z, et al. Temperature characteristics of volume Bragg grating external cavity semiconductor laser working at continuous wave[J]. *Chinese Journal of Lasers*, 2008, 35(1): 27-30.
- [19] Ciapurin I V, Glebov L B, Smimov V I. Modeling of Gaussian beam diffraction on volume Bragg gratings in PTR glass[J]. *Proceedings of SPIE*, 2005, 5742: 183-194.

Research on 795 nm High Power External Cavity Semiconductor Laser

Zhang Wei^{1,2}, Zhong Li^{*}, Zhang Deshuai^{1,2}, Wu Xia¹, Ni Yuxi¹, Liu Suping¹, Ma Xiaoyu¹

¹National Engineering Research Center for Optoelectronic Devices, Institute of Semiconductors, Chinese Academy of Sciences, Beijing 100083, China;

²College of Materials Science and Opto-Electronic Technology, University of Chinese Academy of Sciences, Beijing 100049, China

Abstract

Objective Compared with traditional techniques, magnetic resonance imaging using hyperpolarized inert gas as the contrast agent has greatly improved the quality of lung images. The hyperpolarized inert gas is obtained by means of spin-exchange optical pumping, and pumping the alkali metal rubidium is the key to this process. However, the bandwidth of commercial high-power semiconductor lasers is wide, while the Doppler broadening linewidth of alkali metal atoms is narrow, which leads to low pumping efficiency. To match the pump spectrum width and atomic absorption spectrum width, researchers mainly use the surface grating or volume Bragg grating (VBG) as an external cavity feedback element to develop external cavity semiconductor lasers. In this way, the spectrum width can be narrowed, and the pumping efficiency can be improved to a certain extent. In the existing reports, however, few studies have realized the simultaneous output of lasers with narrow spectrum width and high power. Moreover, under the high power demand, most studies use the laser bar as the internal gain chip, which is exposed to problems such as poor beam quality and great coupling difficulty. Therefore, this work proposes an external cavity semiconductor laser based on a single-tube gain chip. The output performance of the laser can satisfy the narrow spectrum width and have high power in the meanwhile.

Methods VBGs have the characteristics of a high damage threshold and polarization insensitivity. Therefore, this study uses a VBG as the external cavity feedback element and designs the external cavity structure given the performance characteristics of the element. The diffraction efficiency of the VBG is affected by the incident wavelength and the angle of the incident light. According to the diffraction efficiency diagram of the VBG (Fig. 2), a single-tube semiconductor laser with a suitable wavelength is selected as the gain chip. Meanwhile, the front cavity surface of the gain chip can resist reflection after treatment to suppress the influence of the internal cavity mode, and two lenses are added to the external cavity structure to collimate the beam for the best diffraction efficiency of the VBG. Secondly, the completed laser structure is tested, and the laser spectrum and power are monitored and recorded simultaneously. For the understanding of the wavelength stability of the external cavity semiconductor laser, the performance of the laser under different working currents and temperatures is monitored, and the data is analyzed.

Results and Discussions The proposed VBG-based external cavity semiconductor laser can achieve the output power of 6.36 W and a spectrum of 0.036 nm at the operating current of 10 A and the operating temperature of 16 °C (Fig. 4), and the external cavity coupling efficiency reaches 88.5%. Compared with the single-tube semiconductor laser, the proposed semiconductor laser has significantly higher wavelength stability. The drift coefficient of the wavelength to current decreases from 1 nm/A to 0.01 nm/A (Fig. 6), and the temperature drift coefficient decreases from 0.350 nm/°C to 0.005 nm/°C (Fig. 7). In the experiment, it is found that when the difference between the central wavelength of the gain chip and that of the VBG feedback is within the tolerance range, the output from the external cavity semiconductor laser meets the characteristics of narrow spectral width, high power, and stable wavelength. Therefore, for the narrow spectral

width and wavelength stability of the proposed laser in a wider operating current and temperature range, it is necessary to improve the maximum tolerance between the central wavelength of the gain chip and that of the volume Bragg grating feedback. The maximum tolerance of the proposed semiconductor laser is related to the feedback efficiency of the external cavity. It is affected by the reflectance of the front cavity surface of the gain chip, the diffraction efficiency of the VBG, the alignment position of each optical element, the reflectance of the lens, etc.

Conclusions On the basis of the characteristics of VBGs, the structure of the external cavity semiconductor laser is designed in this study. The laser can output high power and narrow spectral width lasers, which solves the difficulty of matching spectral width with atomic absorption spectrum width in the pumping process and improves the pumping efficiency. The wavelength stability of the laser is tested under different operating currents and operating temperatures, and the results show that the laser has good wavelength stability within a certain operating current and temperature range. The relationship between the maximum tolerance between the central wavelength of the gain chip and that of the VBG feedback and the laser performance are presented. The research provides a theoretical and experimental basis for ensuring the stability of the external cavity semiconductor laser in a higher output power range, a larger operating current, and temperature range.

Key words lasers; external cavity semiconductor laser; volume Bragg grating; narrow spectral width; mode locking